NUCLEIC ACID THERAPEUTICS
Volume 31, Number 3, 2021

DOI: 10.1089/nat.2020.0857

Modulating Polymer-siRNA Binding Does Not Promote Polyplex-Mediated Silencing

R. Chauncey Splichal,[1] Joseph A. Gredell,[1,2] Erin B. Vogel,[3,4] Amanda Malefyt,[1,5] Georgina Comiskey,[3,6] Milton R. Smith III,[3] Christina Chan,[1,7] and S. Patrick Walton[1]

The development of delivery vehicles for small interfering RNAs (siRNAs) remains a bottleneck to widespread clinical use. Cationic polymers represent an important class of potential delivery vehicles. In this study, we used alkyne-azide click chemistry to synthesize a variety of cationic poly(propargyl glycolide) backbone polymers to bind and deliver siRNAs. We demonstrated control over the binding interactions of these polymers and siRNAs by varying binding strength by more than three orders of magnitude. Binding strength was found to meet or exceed that of commercially available transfection agents. Our polymers effectively delivered siRNAs with no detectable cytotoxicity. Despite accumulation of siRNAs at levels comparable with commercial reagents, we did not observe silencing of the targeted protein. The implications of our results for future siRNA delivery vehicle design are discussed.

Keywords: cationic polymers, siRNA delivery, poly(propargyl glycolide)

Introduction

Widespread use of small interfering RNAs (siRNAs) in clinical practice will require improvement in the approaches and molecules used for siRNA delivery. Viral and nonviral delivery approaches are being developed. Although viral vectors are generally more efficient [1], safety concerns make further development of nonviral delivery approaches essential. To maximize specific activity of the delivered siRNA, delivery vehicles must be designed to (1) protect siRNAs from degradation by serum nucleases, (2) avoid nontargeted tissues, (3) be endocytosed efficiently by the target cells, (4) allow siRNAs to escape endosomal vesicles, and (5) be cytocompatible [2–4]. To date, most studies that have explored the structure–function relationships of siRNA delivery vehicles have used cell culture screens to identify delivery systems for further investigation *in vivo* [5]. The basic chemistries used in these studies are typically cationic lipids or polymers, as they can readily complex with siRNAs by electrostatic self-assembly.

Cationic polymers provide tunability in designing delivery systems with controlled physical and chemical characteristics [5,6]. The size of cationic polymer–siRNA complexes can be controlled by altering the length of the polymer, the relative amounts of hydrophobic and hydrophilic functionality of the polymer, and the amount of siRNA incorporated in the complex [7]. Charge and charge density can be controlled by varying the chemistry and quantity of cationic monomer or through incorporation of noncharged segments such as poly(ethylene glycol) (PEG) [8]. Incorporation of PEG increased the half-life of siRNA-containing complexes *in vivo* and generally decreased cytotoxicity [8]. In addition, monomers can be selected to add biodegradability and pH sensitivity to block co-polymeric complexes that have been proven effective siRNA delivery vehicles [9–11].

In this work, we sought to identify structure–function relationships for polymeric siRNA delivery vehicles. To achieve structural diversity, we used a postpolymerization modification strategy to synthesize a diverse set of polymers using copper(1)-catalyzed alkyne-azide cycloaddition (CuAAC), a type of ''click'' chemistry, to attach various side chains to a degradable poly(propargyl glycolide) (PPGL) backbone [12–15]. Using this approach allowed us to test polymers with structures/functionalities that mimic polymeric vehicles that have previously proven useful as delivery vehicles and to create and test new structures. We measured the *in vitro* binding of our polymers to short nucleic acids. Subsequently, we tested their utility in delivering siRNAs for silencing in cell culture.

Departments of [1]Chemical Engineering and Materials Science, [3]Chemistry, and [7]Biochemistry and Molecular Biology, Michigan State University, East Lansing, Michigan, USA.
[2]Novozymes Biologicals, Inc, Salem, Virginia, USA.
[4]Dow Chemical Co, Midland, Michigan, USA.
[5]McKetta Department of Chemical & Bioprocess Engineering, Trine University, Angola, Indiana, USA.
[6]ChemTrend LP, Howell, Michigan, USA.

Although we were able to vary binding over a wide range (from 13 μg/mL to >10,000 μg/mL) and successfully delivered fluorescent siRNAs to cells, silencing was not achieved using any of the polymers. Possible explanations for the lack of silencing activity include a lack of release of siRNAs from the endosome, rapid recycling of siRNA complexes out of the cells, or poor delivery of siRNAs to the cells that was masked by accumulation of free fluorophore in the cells.

Materials and Methods

Materials

A detailed list of materials is provided in the Supplementary Data.

Polymer preparation

A Schlenk flask was used to dissolve 40–60 mg of PEG-co-PPGL into dimethylformamide (DMF). Development of the alkyne-functionalized PPGL and the CuAAC procedure were described previously [6]. The desired mole fractions of amine and alkyl sidechains (azide-functionalized) and 24 mole percent sodium ascorbate were then added. The flask was degassed three to four times using a freeze–pump–thaw cycle and backfilled with nitrogen gas. A 0.1 M $CuCl_2 \cdot 2H_2O$ solution was dripped in and stirred overnight at room temperature. The resulting solution was filtered to remove solids. Copper ions were removed by adding Amberlite IRC-748 ion exchange resin beads before filtering again. The DMF was removed *in vacuo*. Remaining polymer was dissolved in a 3:1 water/acetone mixture and dialyzed in a 12–14 kDa MWCO dialysis bag for 2–3 days. The dialysis solvents were removed *in vacuo*. Structures of sidechains are given in Supplementary Fig. S1.

Polymer binding gels

Polymers at varying concentrations were dissolved in 18 MΩ water containing 200 nM 6-carboxyfluorescein-tagged double-stranded DNA (dsDNA) and incubated for 15 min. dsDNA is less susceptible to degradation during the gel electrophoresis process than siRNA, and we have previously shown the use of dsDNA to test polymer binding to be a suitable, cost-effective replacement for siRNA while exhibiting similar binding to the synthesized polymers [16]. A 0.8% agarose gel containing 2 rows of 13 lanes was used for two, simultaneous independent experiments, to separate bound from free dsDNA. The outermost lanes contained no polymer and were used as control intensities for 100% unbound dsDNA. The fraction of bound dsDNA was calculated by dividing the intensity of the free DNA signal in each experimental lane by the intensity of the free DNA signal in the control lane and subtracting the resulting ratio from 1. Calculated fractional binding values from all independent experiments were plotted together. Data were then fit using a modified Hill equation [17] [Equation (1)], where K is the binding coefficient at 15 min, n is a fitted parameter that suggests the presence of cooperative binding, and $[P]$ is the concentration of polymer.

$$\text{Fraction Bound} = \frac{[P]^n}{K^n + [P]^n} \quad (1)$$

The term binding coefficient is used in place of the dissociation constant in the Hill equation, because dissociation constant indicates the polymer–siRNA complexes reached equilibrium. As we only used an incubation period of 15 min before testing binding, we cannot guarantee equilibrium was reached in all cases.

Cell culture

Cells were maintained as described in Portis et al. [16]. In brief, NCI-H1299 (human lung carcinoma) cells expressing enhanced green fluorescent protein (EGFP) with 2-h half-life were obtained from Dr. Jørgen Kjems, University of Aarhus, Denmark [18]. Cells were passaged approximately weekly by trypsinization. Cells were grown in Dulbecco's modified Eagle's medium high glucose supplemented with 10% fetal bovine serum, 1% penicillin/streptomycin, and 1% geneticin and incubated at 37°C, 5% CO_2, 100% relative humidity.

EGFP silencing and cytotoxicity

NCI-H1299-EGFP cells were plated at 20,000 cells per well in 0.1 mL of complete media without antibiotics in a 96-well black side, clear bottom plate and incubated for 24 h. Twenty-four microliters of Opti-Mem was used to complex siRNA and polymer for final concentrations of up to 100 nM siRNA and sufficient polymer to bind the siRNA according to the results of the binding gels. These were mixed and incubated at room temperature for 30 min before transfection. Linear poly (ethylenimine) (LPEI)– and Lipofectamine 2000 (LF2K)–siRNA complexes were prepared to confirm the activity of the siRNA. Transfection solution was left on the cells for 24 h at 37°C, 5% CO_2, and 100% humidity. Before measuring EGFP fluorescence using a Gemini EM fluorescent plate reader (480 nm excitation/525 emission), cells were washed twice with DPBS. Cytotoxicity was determined by comparing the average EGFP signal from 3 wells of a 96-well plate of NCI-H1299-EGFP cells treated with only transfection media with the average EGFP signal from 3 wells treated with transfection media containing polymer. Silencing was measured by comparing the average EGFP signal from 3 wells of a 96-well plate of NCI-H1299-EGFP cells treated with transfection media containing polymer–siRNA complexes with the average EGFP signal from three wells treated with transfection media containing only polymer (no siRNA).

Microscopy

Transfection media was removed, and cells were rinsed before being placed in 0.5 mL of Leibovitz Medium (L-15) media for imaging. An Olympus FluoView 1000 Inverted IX81 microscope with 40× oil objective was used for confocal laser scanning microscopy. EGFP was excited using a 488 nm multi-line Argon laser and detected through a BA505-52 nm emission filter. Dy547-tagged siRNA was excited with a 543 nm HeNe laser and detected through a BA560-IF nm filter. Imaging was performed sequentially using a Kalman average of 2 at the focal plane with the highest intensity EGFP signal.

Results

By using click chemistry to modify PEG-PPGL backbone polymers, we were able to rapidly synthesize 59 unique cationic biodegradable polymers to be complexed with siRNA for transfection of NCI-H1299 cells. The polymers consisted of four structural elements (Fig. 1A). PEG and PGL

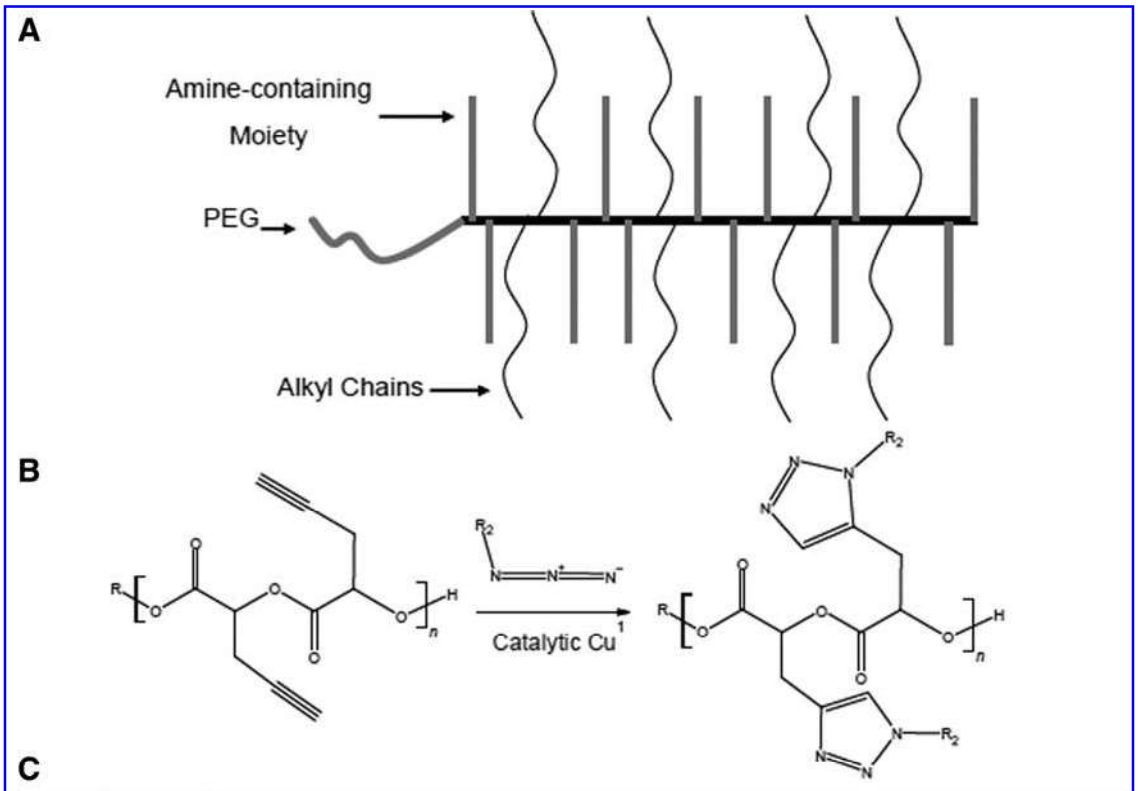

C

Name	Type	Structure
A1	Amine-containing Moiety	
A2	Amine-containing Moiety	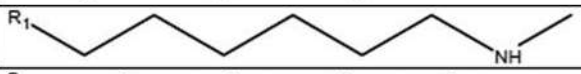
A3	Amine-containing Moiety	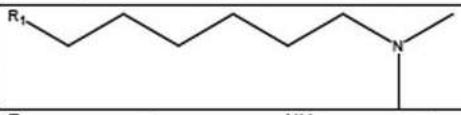
A12	Amine-containing Moiety	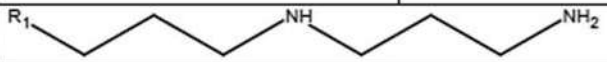
A122	Amine-containing Moiety	
C4	Alkyl Chain	
C10	Alkyl Chain	
C16	Alkyl Chain	
C8π8	Alkyl Chain	
PEG	PEG	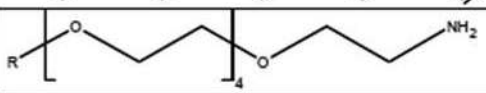

FIG. 1. Synthesis and polymer schematic. **(A)** Schematic showing the general configuration of the polymers. The amine-containing moieties and alkyl sidechains extend radially from the block co-polymer backbone in a brush-like fashion. **(B)** Alkyne-azide reaction used to add functional sidechains to PEG-PPGL block co-polymers. **(C)** The amine-containing moieties and alkyl chains used in this study with associated abbreviation. R indicates a connection along the PPGL backbone, R_1 indicates a connection to the alkyne group on the PPGL backbone, and R_2 indicates a connection to one of the sidechains. Additional structures can be found in the Supplementary Data. PEG, poly(ethylene glycol); PPGL, poly(propargyl glycolide).

Table 1. Name, Structure, and Binding Properties of Vehicles Used for Small Interfering RNA Delivery

		Hill equation			
Name	*Structure*	K *(μg/mL)*	±	n	±
P1	$PEG_8PPGL_{45}(A12_{80}C4_{20})$	140	10	1.0	0.1
P2	$PEG_{115}PPGL_{45}(A12_{80}C4_{20})$	370	40	0.90	0.1
P3	$PEG_8PPGL_{45}(A12_{80}C10_{20})$	31	3	1.4	0.2
P4	$PEG_{115}PPGL_{45}(A12_{80}C10_{20})$	240	20	1.7	0.2
P5	$PEG_8PPGL_{45}(A12_{80}C16_{20})$	13	1	1.9	0.3
P6	$PEG_{115}PPGL_{45}(A12_{80}C16_{20})$	64	1	2.6	0.2
P7	$PEG_{115}PPGL_{45}(A1_{80}C10_{20})$	>10,000			
P8	$PEG_{115}PPGL_{45}(A2_{80}C10_{20})$	>10,000			
P9	$PEG_{115}PPGL_{45}(A3_{80}C10_{20})$	>10,000			
P10	$PEG_{115}PPGL_{45}(A1_{40}A2_{40}C10_{20})$	>10,000			
P11	$PEG_8PPGL_{45}(A12_{80}C8\pi8_{20})$	53	5	1.6	0.2
P12	$PEG_8PPGL_{45}(A122_{80}C10_{20})$	13	1	1.2	0.1
P13	$PEG_8PPGL_{56}[A12_{100}]$	18	1	0.74	0.04
P14	$PEG_8PPGL_{45}(A122_{50}C1EO4C6_{30}X_{20})$	28	4	0.95	0.11
P15	$PPGL_5SSPPGL_5[A12_{100}]$	46	3	0.85	0.04
P16	$PEG_8PPGL_{45}[A12_{50}LC_{50}]$	51	3	1.6	0.1
P17	$PEG_8PPGL_{45}[A12_{100}]$	52	3	1.1	0.1
P18	$PEG_8PPGL_{45}(A12_{90}C10_{10})$	53	5	1.4	0.2
P19	$PEG_8PPGL_{10}(A12_{80}C10_{20})$	53	3	1.4	0.2
P20	$PEG_8PPGL_{45}[A12_{80}C1EO4_{10}ChS_{10}]$	68	8	1.1	0.1
P21	$PEG_8PPGL_{35}(A12_{70}C10_{30})$	71	3	2.4	0.3
P22	$PPGL_{45}(A12_{80}C1EO3C12_{20})$	71	5	2.0	0.3
P23	$PEG_8PPGL_{45}(A12_{70}C10_{30})$	83	5	1.5	0.2
P24	$PEG_8PPGL_{45}(A12_{90}X_{10})$	86	5	1.3	0.1
P25	$PEG_8PPGL_{45}(A12_{60}C10_{40})$	120	20	1.2	0.2
P26	$PEG_8PPGL_{45}(A12_{70}C10_{20}CL_{10})$	140	30	0.60	0.08
P27	$PPGL_5SSPPGL_5[A12_{80}]$	150	10	0.93	0.07
P28	$PEG_{115}PPGL_{45}(A12_{80}C16_{20})$	150	10	1.3	0.2
P29	$PEG_8PPGL_{45}(A12_{80}C1EO4C6_{20})$	170	20	1.1	0.1
P30	$PEG_8PPGL_{45}[A12_{80}C1EO4_{10}ChR_{10}]$	180	10	0.82	0.03
P31	$PEG_8PPGL_{45}(A12_{70}AP_{10}C10_{20})$	200	10	1.4	0.2
P32	$PEG_8PPGL_{45}(A12_{75}C10_{20}G_5)$	240	20	1.7	0.2
P33	$PEG_8PPGL_{45}[A12_{90}Ch_{10}]$	250	20	0.95	0.07
P34	$PEG_{115}PPGL_{45}(A12_{80}X_{20})$	260	20	0.97	0.09
P35	$PEG_{115}PPGL_{45}(A12_{90}C10_{10})$	280	10	1.2	0.1
P36	$PPGL_{30}PEG_{115}PPGL_{30}[A12_{60}C1EO4C6_{40})$	300	40	0.86	0.09
P37	$PEG_8PPGL_{45}(A12_{80}X_{20})$	480	50	0.85	0.08
P38	$PPGL_{50}[A12_{36}C1EO4C6_{64})$	710	60	0.73	0.05
P39	$PPGL_{150}(A12_{70}C10_{30})$	780	30	1.7	0.2
P40	$PEG_8PPGL_{45}[A12_{80}E01C2_{20}]$	920	90	0.73	0.06
P41	$PPGL_{50}[A122_{18}C1EO4C6_{50}X_{32})$	1,200	200	1.3	0.2
P42	$PEG_{115}PPGL_{45}(A12_{90}X_{10})$	1,200	100	1.3	0.2
P43	$PEG_{115}PPGL_{45}(A12_{70}C10_{30})$	1,200	40	3.0	0.4
P44	$PEG_{115}PPGL_{45}(A12_{80}X_{20})$	1,300	200	0.73	0.09
P45	$PPGL_{30}PEG_{115}PPGL_{30}(A12_{50}X_{50})$	1,500	100	0.76	0.06
P46	$PEG_8PPGL_{45}(A12_{70}X_{30})$	2,200	300	0.55	0.04
P47	$PEG_{115}PPGL_{45}(A12_{70}X_{30})$	2,600	200	0.79	0.07
P48	$PEG_{115}PPGL_{45}[A12_{90}Ch_{10}]$	3,200	1000	0.40	0.06
P49	$PEG_{115}PPGL_{45}(A12_{50}X_{50})$	4,100	500	0.65	0.65
P50	$PEG_8PPGL_{45}(A12_{18}C1EO4C6_{50}X_{22})$	4,300	500	0.86	0.09
P51	$PEG_{115}PPGL_{45}(A12_{60}C10_{40})$	>10,000			
P52	$PEG_{115}PPGL_{45}(A12_{50}C10_{50})$	>10,000			
P53	$PPGL_{55}(C1EO4_{80}C10_{20})$	>10,000			
P54	$PEG_8PPGL_{45}(A2_{80}C10_{20})$	>10,000			
P55	$PEG_8PPGL_{45}(A3_{80}C10_{20})$	>10,000			
P56	$PEG_8PPGL_{45}(A12_{70}X_{30})$	>10,000			
P57	$PEG_{115}PPGL_{45}(A1_{70}C10_{30})$	>10,000			
P58	$PEG_8PPGL_{67}[A12_{80}C2EO2C2_{10}]$	>10,000			
P59	$PEG_8PPGL_{45}[A12_{50}CA_{50}]$	>10,000			
PLL		0.36	0.06	0.92	0.16
LPEI25		3.0	0.4	1.8	0.4
LPEI2.5		3.2	0.6	1.1	0.2
LF2K		4.9	0.7	0.94	0.12
BPEI		38	2	2.6	0.3

BPEI, branched poly(ethylenimine); LF2K, Lipofectamine 2000; LPEI, linear poly(ethylenimine); PEG, poly(ethylene glycol); PLL, poly-L-lysine; PPGL, poly(propargyl glycolide).

were linked and served as the polymer backbone. ''Click'' chemistry (Fig. 1B) was used to functionalize the backbone with amine-containing or alkyl sidechains (Fig. 1C). PEG length was varied, with each polymer having a PEG segment length of 0, 8, or 115 repeat units (Table 1). PGL length was also varied from 5 to 150 repeat units. The amine functional groups added to the PGL backbone were either primary, secondary, tertiary, or a combination of primary and secondary amines (Fig. 1C). Alkyl sidechains ranged from 4 to 16 carbons in length.

Polymer–nucleic acid complex formation was measured using a gel-shift assay (Fig. 2). Binding coefficients, K, varied from 13 μg/mL to >10,000 μg/mL (Table 1). We also tested binding for a number of commercially available siRNA delivery systems that have demonstrated silencing [poly-L-lysine (PLL), LPEI, LF2K, and branched poly(ethylenimine) (BPEI)] and found these to have binding coefficients between 0.36 and 38 μg/mL. The modified Hill equation contains a parameter, n, that can relate to cooperativity of binding. A value of $n > 1$ suggests that binding of siRNA to a polymer enhances further siRNA binding to the polymer [17]. We observed no trends relating n to structural elements (Table 1). From our binding results, we showed that more PEG monomers per polymer decreased binding between dsDNA and the polymer (Table 1; compare P1 with P2, P3 with P4, and P5 with P6). Polymers with sidechains containing primary amines (P7), secondary amines (P8), tertiary amines (P9), or a combination of primary and secondary amines on separate sidechains (P10) were unable to achieve binding coefficients <10,000 μg/mL; however, sidechains containing both primary and secondary amines on the same branch (P4 and polymers containing A12, A112, or A122) had measurable binding coefficient. In addition, our results demonstrated that longer alkyl sidechains resulted in lower binding coefficients (stronger binding interactions) [compare P1 (4 carbon alkyl chain), P10 (8 carbon alkyl chain), P3 (10 carbon alkyl chain), and P5 (16 carbon alkyl chain)].

Confocal laser scanning microscopy was used to test the ability of our polymers to deliver siRNAs. A representative example, polymer P3, delivered siRNA to NCI-H1299 cells (Fig. 3); however, despite accumulation at levels comparable with those achieved with LF2K (Fig. 3, compare C and I), the siRNAs did not reduce the expression of EGFP. Indeed, none of the synthesized polymers led to a statistically significant decrease in EGFP, regardless of the strength of the binding interaction between the siRNA and polymer.

Discussion

For siRNAs to accumulate in cells, delivery vehicles must bind them and protect them from nuclease degradation during delivery. We have shown increasing PEGylation of polymers impairs their binding with dsDNA/siRNA, whereas combining primary and secondary amines, increasing the number of amines, and increasing the length of alkyl sidechains improves binding. It has been shown previously that PEGylation decreases binding affinities of nucleic acid/polymer complexes by charge shielding [8]. Of interest, isolated primary, secondary, and tertiary amines all have pK_a values above physiological pH; therefore, differences in pK_a among the amine classes do not account for the differences in binding. The inclusion of two nearby amines in the A12 sidechain potentially allowed for multiple binding sites between the siRNA and polymer, stabilizing the electrostatic interaction [19].

Binding of a polymer to siRNAs can be sterically limited [20]. Incorporation of alkyl chains can produce nanoparticles with a hydrophobic core with cationic arms extending into the hydrophilic solution [21]. These arms are then more spatially available to conform to the siRNA, improving binding. Amphiphilic polymer nanoparticles can also form micelle-like conformations surrounding siRNAs [8]. The inclusion of a double bond in P10 impairs binding compared with P5 with the same number of carbons (Table 1), indicating that hydrophobic packing may be crucial for the

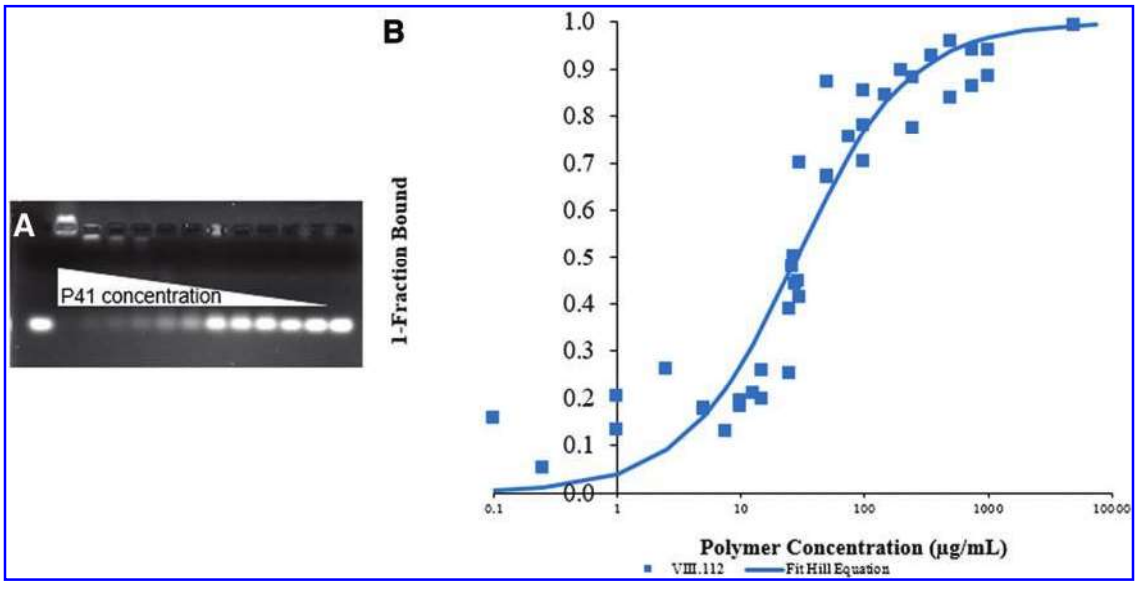

FIG. 2. Gel-shift Analyses. **(A)** DNA binding gel for P41 depicting the change in intensity of free DNA as the amount of polymer increases from *right* to *left*. **(B)** The graph shows results from four independent binding gels of P41 with the modified Hill equation fit ($K = 28.3$ μg/mL, $n = 0.95$). Color images are available online.

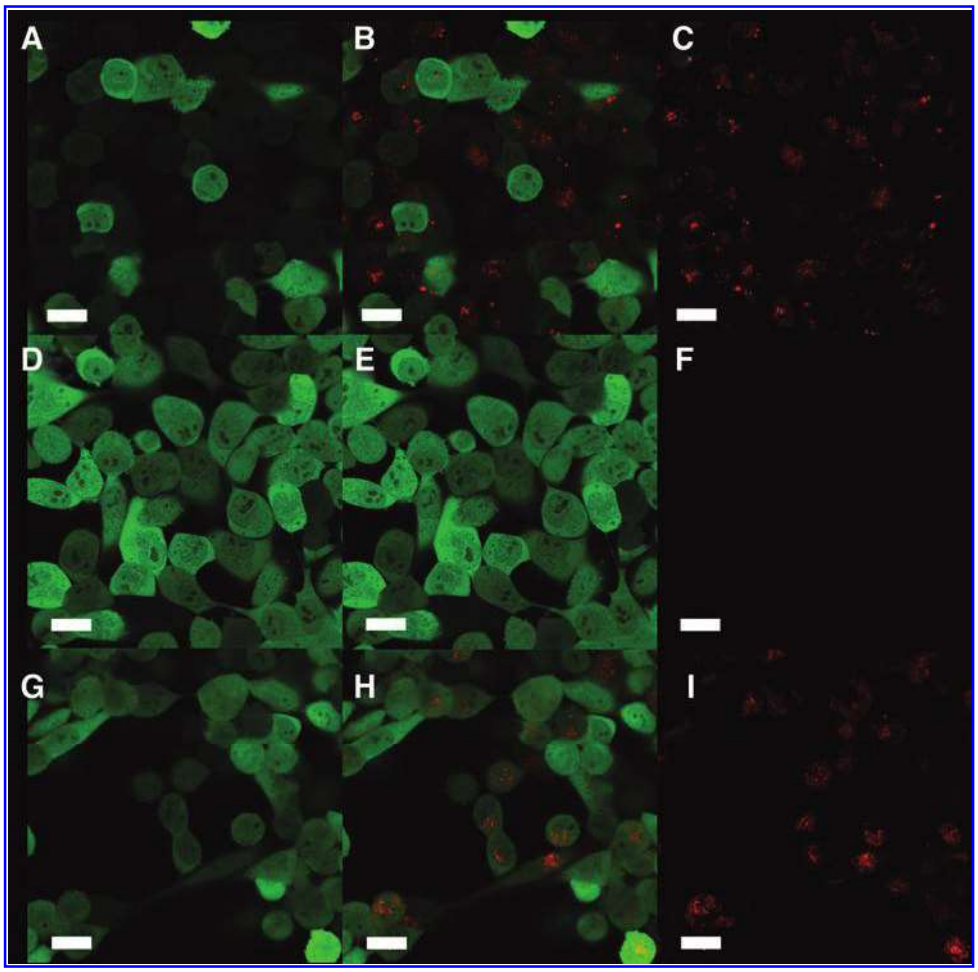

FIG. 3. siRNA accumulation and silencing. Shown are the delivery of Dy547-siRNA and silencing of EGFP in NCI-H1299-EGFP cells, all scale bars are 20 μm. **(A–C)** Transfection using LF2K at 1 μg/mL and 100 nM Dy547-siRNA for 24 h, where **A** is the *green* channel, **C** is the *red* channel, and **B** is the overlay of **A** and **C**. **(D–F)** Untreated, control NCI-H1299-EGFP cells. **(G–I)** Transfection using 50 μg/mL of P3 and 100 nM Dy547-siRNA. Average EGFP intensity in the cells receiving siRNA through P3 did not change compared with the control cells as measured by plate reader. The cytotoxicity of the polymers was tested by comparing EGFP expression in cells treated with the polymer in the absence of siRNA and untreated control EGFP cells; no statistically significant toxicity was seen for any polymer at the concentration at which it was tested. EGFP, enhanced green fluorescent protein; LF2K, Lipofectamine 2000; siRNA, small interfering RNA. Color images are available online.

enhanced binding observed with longer alkyl sidechains. This further supports our hypothesis that these polymers form a micellar structure.

It is notable that many of our polymers had binding interactions of similar strength to those of the commercial vehicles. Moreover, our polymers successfully delivered siRNAs into cells at comparable concentrations. Nonetheless, none of the polymers tested was able to lead to silencing of EGFP. One possible explanation for the lack of efficacy of the polymers is the absence of secondary and tertiary amines, which can buffer solutions as low as pH = 3 and therefore may lead to the proton sponge effect and endosomal rupturing to release siRNAs [22,23]. Amphiphilic siRNA delivery vehicles have also been shown to disrupt endosomal membrane stability and thereby allow siRNAs to enter the cytoplasm [24]. To disrupt the membrane, delivery vehicles must be near neutral charge at endosomal pH to avoid electrostatic exclusion from the membrane [24]. However, our polymers are likely too positively charged to interact with the membrane in this manner. Another possible explanation for the lack of effective delivery by our polymers is that endosomes containing the polymers are quickly tagged for recycling or degradation, not allowing for sufficient time to release their cargo [25]. We have previously shown that accumulation of siRNAs in cells does not directly correlate to the degree of silencing achieved [26]. Thus, it is possible that the siRNAs delivered by our polymers may have been endocytosed for recycling but precluded from reaching the cytoplasm and initiating RNAi. Finally, it is possible that the Dy547 fluorophore detaches from the siRNA before cellular internalization and enters either alone or with the PPGL nanoparticle. It is unclear why this would be more likely to occur during delivery by the polymers than by LF2K, but, if it were the case, our levels of delivered siRNA may be insufficient to achieve silencing.

The development of effective and safe delivery systems remains a limiting step in the clinical application of siRNAs. Our polymers offer a unique opportunity to assess the vehicle characteristics that influence downstream siRNA activity because of their facile modification by click chemistry. The benefits of having multiple classes of amines incorporated into one polymer remain unclear but could contribute to better binding affinity or an increased buffering capacity. The incorporation of higher molecular weight alkyl sidechains requires future investigation to find the length of alkyl chain that optimizes binding with siRNA without impairing solubility or increasing size. Finally, it will be important to understand how alkyl sidechain length impacts stability, conformation, and, ultimately, the delivery effectiveness of polymeric vehicles for siRNAs.

Acknowledgments

The authors thank the members of the Cellular and Biomolecular Laboratory for their advice and support. The authors acknowledge the contributions to this work of the late Gregory L. Baker, our mentor, colleague, and friend, who was an exceptional polymer scientist and instrumental in the initial design and execution of this collaborative work.

Author Disclosure Statement

No competing financial interests exist.

Funding Information

This work was supported by Michigan State University, the National Science Foundation [CBET1510895, 1547518, 1802992], and the National Institutes of Health [GM089866, T32GM092715 to R.C.S.].

Supplementary Material

Supplementary Data
Supplementary Figure S1

References

1. Oliveira S, G Storm and R Schiffelers. (2006). Targeted delivery of siRNA. J Biomed Biotechnol 2006:1–9.
2. Angart P, D Vocelle, C Chan and SP Walton. (2013). Design of siRNA therapeutics from the molecular scale. Pharmaceuticals 6:440–468.
3. Setten RL, JJ Rossi and S Han. (2019). The current state and future directions of RNAi-based therapeutics. Nat Rev Drug Discov 18:421–446.
4. Kanasty R, JR Dorkin, A Vegas and D Anderson. (2013). Delivery materials for siRNA therapeutics. Nat Mater 12: 967–977.
5. O'Mahony AM, J Ogier, S Desgranges, JF Cryan, R Darcy and CM O'Driscoll. (2012). A click chemistry route to 2-functionalised PEGylated and cationic β-cyclodextrins: co-formulation opportunities for siRNA delivery. Org Biomol Chem 10:4954–4960.
6. Jiang X, EB Vogel, MR Smith and GL Baker. (2008). ''Clickable'' polyglycolides: tunable synthons for thermoresponsive, degradable polymers. Macromolecules 41: 1937–1944.
7. Howard KA, UL Rahbek, X Liu, CK Damgaard, SZ Glud, M Andersen, MB Hovgaard, A Schmitz, JR Nyengaard, F Besenbacher and J Kjems. (2006). RNA interference in vitro and in vivo using a novel chitosan/siRNA nanoparticle system. Mol Ther 14:476–484.
8. Nelson CE, JR Kintzing, A Hanna, JM Shannon, MK Gupta and CL Duvall. (2013). Balancing cationic and hydrophobic content of PEGylated siRNA polyplexes enhances endosome escape, stability, blood circulation time, and bioactivity in vivo. ACS Nano 7:8870–8880.
9. Patil Y and J Panyam. (2009). Polymeric nanoparticles for siRNA delivery and gene silencing. Int J Pharm 367:195–203.
10. Tsai LR, MH Chen, C Te Chien, MK Chen, FS Lin, KMC Lin, YK Hwu, CS Yang and SY Lin. (2011). A single-monomer derived linear-like PEI-co-PEG for siRNA delivery and silencing. Biomaterials 32:3647–3653.
11. Zhu C, S Jung, S Luo, F Meng, X Zhu, TG Park and Z Zhong. (2010). Co-delivery of siRNA and paclitaxel into cancer cells by biodegradable cationic micelles based on PDMAEMA-PCL-PDMAEMA triblock copolymers. Biomaterials 31:2408–2416.
12. Kolb HC, MG Finn and KB Sharpless. (2001). Click chemistry: diverse chemical function from a few good reactions. Angew Chem Int Ed 40:2004–2021.
13. Günay KA, P Theato and HA Klok. (2013). Standing on the shoulders of hermann staudinger: post-polymerization modification from past to present. J Polym Sci Part A Polym Chem 51:1–28.
14. Rostovtsev VV, LG Green, VV Fokin and KB Sharpless. (2002). A stepwise huisgen cycloaddition process: copper(I)-catalyzed regioselective ''ligation'' of azides and terminal alkynes. Angew Chem Int Ed 41:2596–2599.
15. Haldón E, MC Nicasio and PJ Pérez. (2015). Copper-catalysed azide-alkyne cycloadditions (CuAAC): an update. Org Biomol Chem 13:9528–9550.
16. Portis AM, G Carballo, GL Baker, C Chan and SP Walton. (2010). Confocal microscopy for the analysis of siRNA delivery by polymeric nanoparticles. Microsc Res Tech 73: 878–885.
17. Hill A. (1910). The possible effects of the aggregation of molecules of haemoglobin on its dissociation curves. J Physiol 40:iv–vii.
18. Liu X, KA Howard, M Dong, M Andersen, UL Rahbek, MG Johnsen, OC Hansen, F Besenbacher and J Kjems. (2007). The influence of polymeric properties on chitosan/siRNA nanoparticle formulation and gene silencing. Biomaterials 28:1280–1288.
19. Kakizawa Y and K Kataoka. (2002). Block copolymer micelles for delivery of gene and related compounds. Adv Drug Deliv Rev 54:203–222.
20. Kim HJ, K Miyata, T Nomoto, M Zheng, A Kim, X Liu, H Cabral, RJ Christie, N Nishiyama and K Kataoka. (2014). SiRNA delivery from triblock copolymer micelles with spatially-ordered compartments of PEG shell, siRNA-loaded intermediate layer, and hydrophobic core. Biomaterials 35:4548–4556.
21. Zhu J, A Tang, LP Law, M Feng, KM Ho, DKL Lee, FW Harris and P Li. (2005). Amphiphilic core-shell nanoparticles with poly(ethylenimine) shells as potential gene delivery carriers. Bioconjug Chem 16:139–146.
22. Boussif O, F LezoualC'H, MA Zanta, MD Mergny, D Scherman, B Demeneix and JP Behr. (1995). A versatile vector for gene and oligonucleotide transfer into cells in culture and in vivo: polyethylenimine. Proc Natl Acad Sci U S A 92:7297–7301.

23. Benjaminsen RV, MA Mattebjerg, JR Henriksen, SM Moghimi and TL Andresen. (2013). The possible ''proton sponge'' effect of polyethylenimine (PEI) does not include change in lysosomal pH. Mol Ther 21:149–157.
24. Kandil R, Y Xie, R Heermann, L Isert, K Jung, A Mehta and OM Merkel. (2019). Coming in and finding out: blending receptor-targeted delivery and efficient endosomal escape in a novel bio-responsive siRNA delivery system for gene knockdown in pulmonary T cells. Adv Ther 2: 1900047–1900061.
25. Sahay G, W Querbes, C Alabi, A Eltoukhy, S Sarkar, C Zurenko, E Karagiannis, K Love, D Chen, et al. (2013). Efficiency of siRNA delivery by lipid nanoparticles is limited by endocytic recycling. Nat Biotechnol 31:653–658.
26. Vocelle D, C Chan and SP Walton. (2020). Endocytosis controls small interfering RNA efficiency: implications for small interfering RNA delivery vehicle design and cell-specific targeting. Nucleic Acid Ther 30:22–32.

Address correspondence to:
S. Patrick Walton, ScD
Department of Chemical Engineering and Materials Science
Michigan State University
428 South Shaw Lane, Room 3249
Engineering Building
East Lansing, MI 48824-1226
USA

E-mail: spwalton@egr.msu.edu

Received for publication February 10, 2020; accepted after revision July 2, 2020; Published Online: July 29, 2020.